Practical CFD Simulations of Wind Tunnel Tests

Dilip Banerjee, Scott Hemley, Randall McDermott, DongHun Yeo, Frank Lombardo, and Marc Levitan

Engineering Laboratory, National Institute of Standards and Technology (NIST), Gaithersburg, MD

ABSTRACT

Computational fluid dynamics (CFD) has the potential of replacing wind tunnel testing in many wind engineering applications. Validated CFD software could enable engineers to calculate wind effects on buildings for which no aerodynamic information is currently available. However, the use of CFD for structural engineering applications is limited mainly because of its prohibitive computational resource requirements. This is due in part to the need to simulate the imperfect spatial coherence of the low-frequency turbulent fluctuations in the incoming atmospheric boundary layer (ABL) flow. A methodology is needed that would remove this barrier. In addition, it is desirable to develop software capable of readily incorporating features specific to the simulation of aerodynamic effects on bluff bodies. For this reason NIST's open source Fire Dynamics Simulator (FDS) is being adapted for wind engineering applications. FDS numerically solves the spatially filtered form of the Navier-Stokes equations appropriate for incompressible flow, a technique known as large-eddy simulation (LES).

In a first phase of this research, FDS has been used to compare data obtained from University of Western Ontario (UWO) wind tunnel tests on a 1:100 scale model of the Texas Tech University's Wind Engineering Research Field Laboratory building (prototype dimensions: 9.1 m (L) $\times$ 13.7 m (B) $\times$ 4 m (H)). Pressure taps or ports along four lines on the model are chosen for comparison with FDS output. FDS is used to simulate flow in the wind tunnel and compare pressures on the building at several locations for varying angles of attack. Mesh refinement is also varied in the numerical simulation. Overall, the results from the FDS simulations fit the experimental data well.

The paper discusses in detail the validation of wind pressure results, as well as issues being addressed to incorporate simplified ABL flow simulations in FDS. Additional issues such as modeling of non-orthogonal building surfaces and numerical issues associated with modeling flow in the wind tunnel are discussed.

1. INTRODUCTION

Computational Fluid Dynamics (CFD) is a strong candidate for replacing wind tunnel testing in many wind engineering applications. The use of CFD for structural engineering applications is limited, however, by its prohibitive computational resource requirements. The main contributor to the large computational time is the perceived need to simulate the imperfect spatial coherence of the low-frequency turbulent fluctuations in the incoming atmospheric boundary layer (ABL) flow. A methodology that would successfully remove this barrier to the use of CFD by engineers is needed because of high costs, long lead times, gross Reynolds number violation, and large simulation uncertainties inherent in wind tunnel testing.

CFD could enable engineers to calculate with ease wind effects on many building geometries for which no aerodynamic information is currently available. In addition, an adaptation of the CFD procedure for tall buildings is possible, wherein rapid and effective estimates of wind effects would allow the assessment of the relative aerodynamic performance of buildings with different geometric characteristics, e.g., buildings with square cross section and sharp corners vs. buildings with square cross section and chamfered corners.

An effective CFD modeling procedure applicable to civil engineering structures will help develop critically-needed standard provisions allowing improved design of new buildings and retrofitting of existing buildings subjected to wind loads. In a first phase of the development of such a procedure, the NIST Fire Dynamics Simulator (FDS) has been adapted for use in wind engineering applications (FDS version 6, Ref [1]), and has been used to model flow in a wind tunnel. Computed and experimental pressures are compared to verify the CFD simulations.

In the next sections, FDS simulations are discussed in detail and their results are compared to experimental data. The comparisons indicate that FDS has an excellent potential for being adapted for wind engineering applications.

2. FIRE DYNAMICS SIMULATOR

FDS numerically solves the spatially filtered form of the Navier-Stokes equations appropriate for incompressible flow using a technique known as large-eddy simulation (LES). The mass, momentum, and energy equations are discretized by finite differences and a numerical solution is obtained as a function of time on a 3-D rectilinear grid. Turbulence is treated by means of a dynamic eddy viscosity model. The wall stress is modeled by a logarithmic wall function.

All FDS calculations must be performed within a domain that is made up of right parallelepipedic volumes called meshes. Each mesh is divided into rectilinear volumes. The number of cells depends on the desired resolution of the computed flow dynamics. The wind tunnel is discretized with an orthogonal grid. The 1:100 scale model of the Texas Tech University Wind Engineering Research

Field Laboratory building (dimensions: 9.1 m (L) × 13.7 m (B) × 4 m (H)) is defined as an "Obstruction" in the FDS input file [1]. A parallelized version of the FDS software was used to model the flow for better computational efficiency.

2.1 FDS Model of the Wind Tunnel Tests

The experimental wind tunnel model developed at UWO is shown in Figure 1. After developing the overall computational domain for this Wind Tunnel in FDS, mesh characteristics were determined for two levels of mesh refinement: coarse and fine. FDS cases were created in order
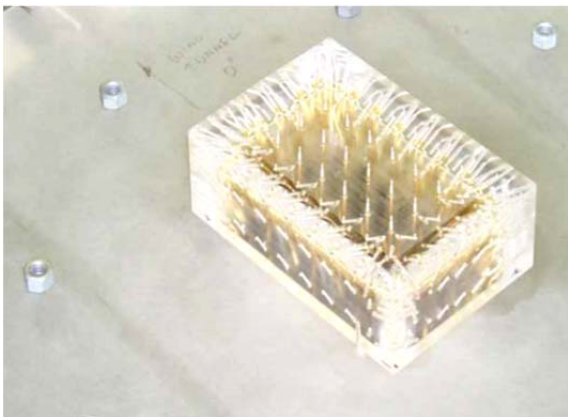

Figure 1 1:100 wind tunnel model at UWO [2].

to simulate the UWO wind tunnel tests for various angles of attack at these two levels of mesh refinement. Pressure taps along four lines on the UWO building model, shown in Figure 2, were chosen for comparison with FDS output. Lines of "output devices or ports" were created in FDS at the same locations and the experimental data were plotted against the FDS output. The experiments were conducted at various angles of attack on the model, but first the tests conducted at 180° and 270° were used for comparisons with simulated results. These angles simplify the simulations in FDS because oblique angles complicate the calculations at the boundaries of the computational domain. All of the FDS cases use the same computational domain, which is a 1.12 m × 0.56 m × 0.28 m space split into eight uniform meshes. This domain size was chosen because it is large enough that the walls do not affect the wind flow and small enough that the simulations are not too time consuming. The domain is shown with the FDS model in Figure 3.
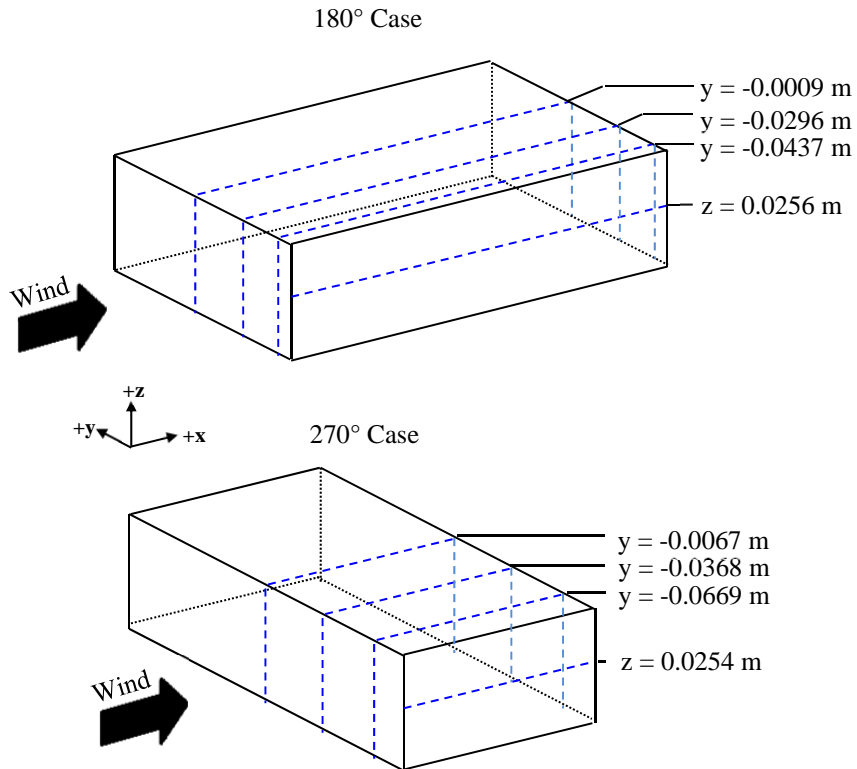
180° Case

y = -0.0009 m
y = -0.0296 m
y = -0.0437 m

z = 0.0256 m

+z
+y   +x

Wind

270° Case

y = -0.0067 m
y = -0.0368 m
y = -0.0669 m

z = 0.0254 m

Wind

Figure 2 Positions of pressure taps used in 180° and 270° cases at model (1:100) scale. The origin of the coordinate axes is at ground level at the center of the building in both cases.
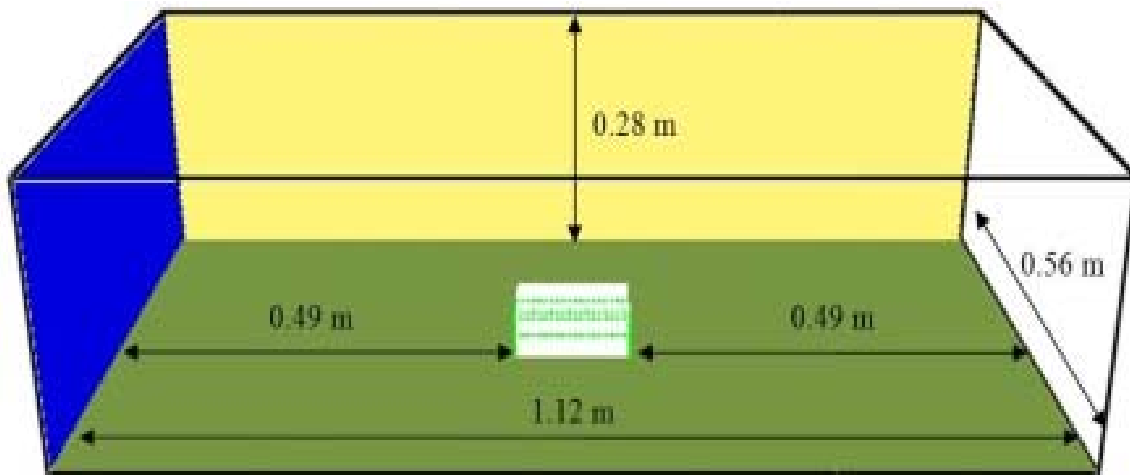
0.28 m

0.56 m

0.49 m   0.49 m

1.12 m

Figure 3 Computational domain for UWO simulation with building model in the center. The blue surface is the inlet, the green surface is the ground, the yellow surface is the wall, and the white surface is the outlet. The green points on the building are the devices that measure the pressure coefficients.

The domain is composed of a different size of cubic cells for each level of mesh refinement. In the coarser cases, each of the eight meshes is divided into 32 cells in each coordinate direction and each cell is a 0.00875 m cube. In the finer cases, the cells are half as large in each direction, yielding eight times as many cells. It was important to make the cells cubic in order to accurately represent turbulence in the flow simulation. This is because small scale turbulence can be resolved better with more accuracy and reliability when using cubic cells. Furthermore, non-cubic cells increase the likelihood of discretization error thereby enhancing the possibility of not resolving small scale turbulence correctly. One consequence of using cubic cells is that the size of the building model had to be slightly modified (less than 5% change in physical dimensions) to be a multiple of the cell size in each direction, but accurate flow calculations were more important in this simulation than slight variations in the building size. These variations could be reduced by further mesh refinement.

For the case of oblique angle flows, the computational domain was slightly modified. The domain was widened so that it was square in the *x* and *y* dimensions (ranging from -0.56 to 0.56 m in *x* and *y*), two of the boundaries were set as inlet vents, and the two opposite boundaries were set to "open" condition. The same mesh resolution was used after widening the domain, so the whole domain was expanded to 16 computational meshes instead of 8 and the simulations became more computationally expensive as a result.

2.2 Input of Experimental Data into FDS Model

2.2.1 Inlet Velocity

The incoming flow assigned at the inflow boundary was characterized by its mean wind speed profile and turbulent fluctuations. For consistency with the UWO experiments, the mean wind speed profile was modeled by the power law:

$$U(z) = 9.144 \left(\frac{z}{0.0396} \right)^{p} \quad \text{[m/s]}$$

where the 9.144 m/s is the reference wind speed at the 0.0396 m roof height of the model, and the power law exponent $p = 0.1173$ was fitted to the experimental data.

2.2.2 Turbulence Parameters

The synthetic turbulence parameters were set for the inlet surface. The fluctuations were generated by the Synthetic Eddy Method (SEM) based on the work of Jarrin [3]. The desired value of N_EDDY (the number of eddies generated at the inlet) was the largest possible value that would not slow down the simulation. This value was determined by running a number of simulations for the same time while varying the N_EDDY input and recording the total run time. The other turbulence parameters, L_EDDY (characteristic eddy length) and

REYNOLDS_STRESS, were set based on the turbulence intensity data from the UWO experiments. The Reynolds stresses were found by multiplying the turbulence intensity in each direction by the wind velocity at roof height to determine the root mean square of the velocity fluctuations, and then squaring the root mean square values.

2.2.3 Other Boundary Conditions

The side walls and roof were set to the free-slip condition in FDS. For the ground, the roughness length was specified in the experimental data to be 0.01 m at full scale. Therefore, the ground was set to a roughness value of 0.0001 m in the model. The building surface was set to the same conditions as the ground because setting a roughness length in FDS changes the wall stress model used in the calculations. Finally, the outlet of the wind tunnel was set to an "open" boundary condition, where pressure is set to the ambient pressure.

After setting the boundary conditions, a test FDS case was created to confirm that the flow field in the simulation matched the desired inputs. Four planes of 42 "output devices" along the length of the domain were used to write out computational results. These planes are located just inside the inlet and at one quarter, one half, and three quarters of the total length. The devices output time series of the wind velocity in each coordinate direction throughout the simulation, and the resulting velocity data were used to determine the characteristics of the wind flow from the inlet as it varies in space and time. As expected, the velocity profile was found to match the inlet condition closely at each of the four planes.

The variable $y^+ = u_* y / \nu$ (where u_* is the friction velocity at the wall, y is the distance to the wall, and ν is the kinematic viscosity of the fluid) is a non-dimensional wall distance for a wall-bounded flow. It was used as a measure of mesh refinement and was written in output boundary files to visualize the values on the surface of the building. The grid resolution in these FDS simulation cases was determined to be sufficient because the y^+ (a non-dimensional distance) values never exceeded 150 in the FDS simulation obtained using either the coarse or fine meshes. y^+ values are dependent on turbulence model wall laws and a value of 150 means that the first grid point is well within the logarithmic region. Four lines of devices were created on the building to measure and output values, and a boundary file was output to visualize the pressure coefficient. The devices were positioned on the building as shown in Figure 3, and measured the mean and root mean square values of the pressure coefficient at each point over the simulation time. The pressure coefficient measurements were referenced to the velocity at roof height to be consistent with the experimental data. Overall, the results from the FDS simulations fit the experimental data well.

3. FDS SIMULATIONS

In this section, the FDS simulations are discussed first to ensure that the predicted results follow expected results obtained in typical wind tunnel experiments. Then, predicted FDS results are compared with available measured data obtained from wind tunnel experiments. FDS analyses were run for several angles of attack used in wind tunnel tests.

3.1 Verification of FDS

One of the important features of the wind turbulence is its spectrum. The normalized reduced spectrum is defined as nSu/u^*, where n is frequency, S is the spectral density of wind speed, u is the mean wind speed, and u^* is the friction velocity that represents shear strength at the boundary layer [4]. The normalized spectrum is plotted against the normalized or reduced frequency defined as $f = n\,z/u(z)$, also known as similarity coordinate (ratio of height to wavelength). A wind spectrum plot is shown in Figure 4.
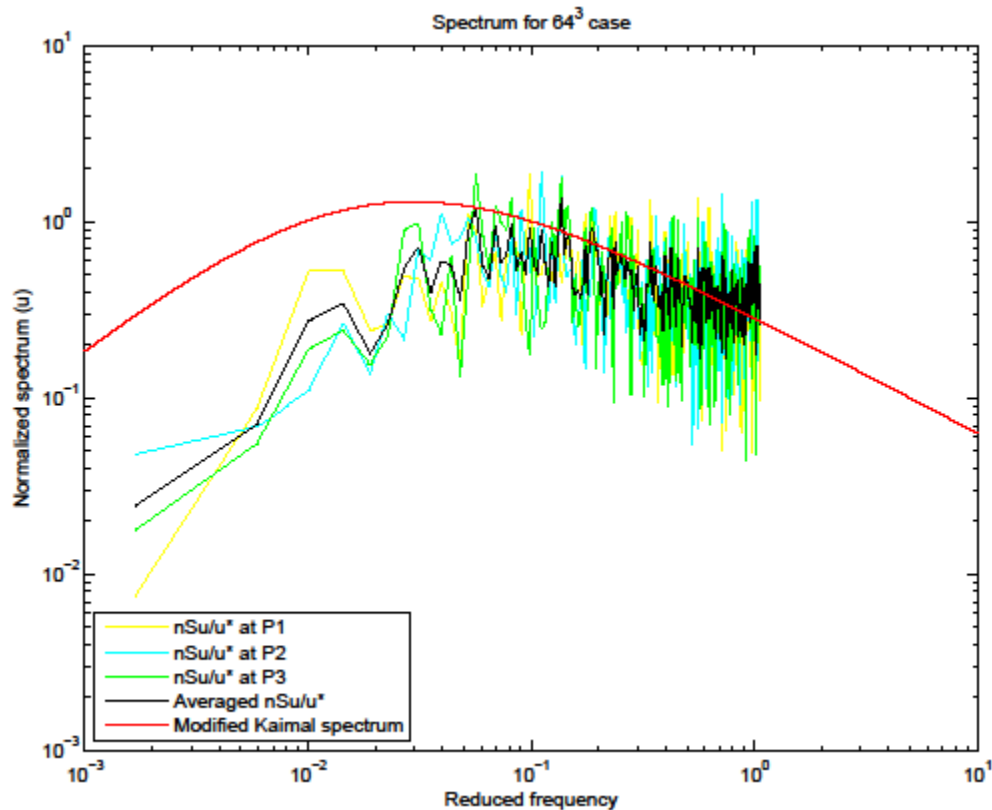

Figure 4. Computed normalized wind spectrum vs. reduced frequency obtained with FDS simulation with fine mesh (64^3 cells per mesh).

Points P1, P2, and P3 shown in Figure 4 are located at roof height of the building in the middle of the computation domain (at position $L/2$ if L is defined as the length of the domain). Similar spectra have been obtained for other angles of attack, and show similar trends. It can be seen that

the empirical formula in Modified Kaimal Spectrum provides a good match with computed values in the high f   uency range (f>0.2), as expected [4]. Such empirical formula are often conservatively valid in the high frequency range [4]. Another useful verification exercise was to plot the turbulence intensity along the length of the simulated wind tunnel as a function of height. One such graph is shown in Figure 5, which plots turbulence intensities in the z direction at inlet, at $L/4$ (L=length of Wind tunnel), $L/2$, and $3L/4$. The plot shows that the turbulence intensity reaches a maximum at a short distance from the floor for all four locations, after which it drops steadily with increase in height, as expected. Also, the turbulence intensity is maximum at the inlet, as should indeed be the case. The turbulence intensity at the location of the model was approximately equal to the value achieved in the University of Western Ontario wind tunnel at 0.1 m above the tunnel floor (corresponding to 10 m full scale), see Ho et al. (2003) [2].
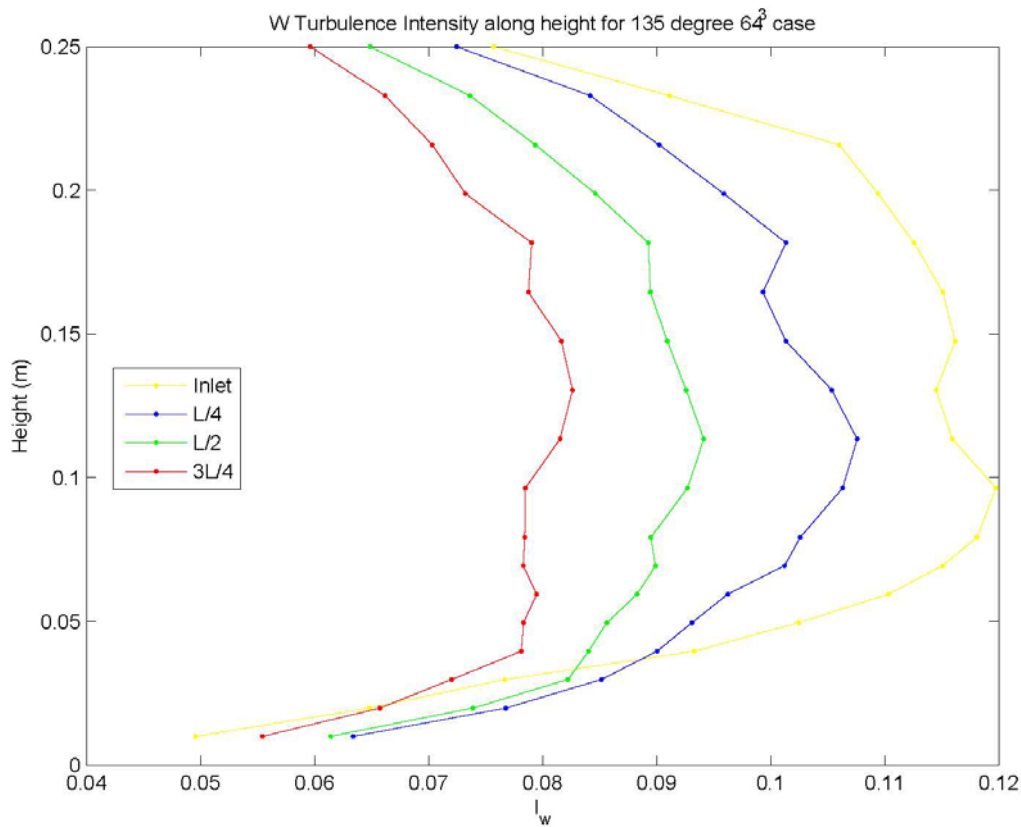

Figure 5. Computed turbulence intensity (in z-direction) along height at four locations along the length of the wind tunnel obtained using FDS simulation with fine mesh for wind angle of attack 135˚.

3.2 Pressure Coefficients

Measured pressure coefficient data were obtained from the wind tunnel tests conducted at UWO. Four lines of "output devices" were created on the building (see Figure 2) to output pressure coefficient values computed by FDS to compare with experimental measurements. The mean,

maximum, minimum, and root mean square values of the pressure coefficient at each point ("output device") were written by FDS over the entire simulation time. Again, the pressure coefficient measurements were referenced to the velocity at roof height to be consistent with the experimental data. Mean pressure coefficients (computed and experimental) at pressure taps located at a given *y*-coordinate for a 180° angle of attack are shown in Figure 6. Error bars were
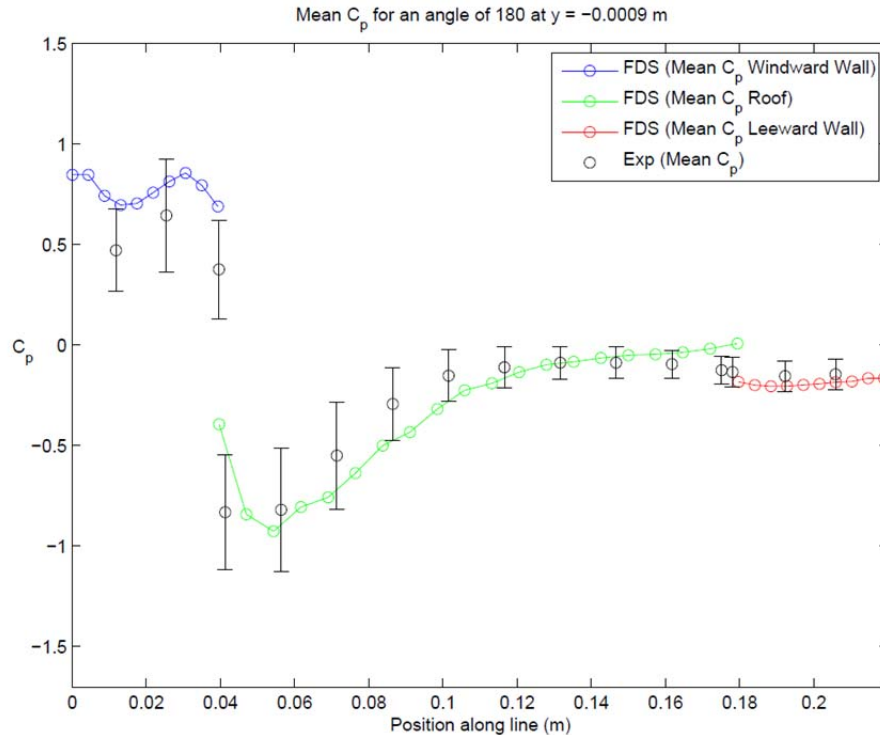

Figure 6 FDS output plotted against experimental data for the line of devices at y = -0.0009 m in the 180° case.

written using root mean squares of fluctuating velocity (e.g., one standard deviation). The results show reasonably good agreement. Similar agreement was obtained for other angles of attack as well, including for wind directions not perpendicular to the faces of the building model). It is evident from Fig. 6 that FDS simulated values were close to the mean of experimental values except at the windward wall where they appear to be closer to the high end of the range of experimental values.

While the results were accurate for mean pressures, it was found that FDS results do not match maximum and minimum pressures especially at the windward wall, (see Figure 7 (a) and (b),) The reason behind this is unclear at this point.

Apart from wind directions perpendicular to the face of the building, cornering flow cases were investigated for angles of attack of 30, 35, 40, and 135° in FDS. The pressure coefficients plots show that, just like the perpendicular cases, in all cases FDS predicts mean values reasonably accurately but the maximum and minimum values are not matched well.
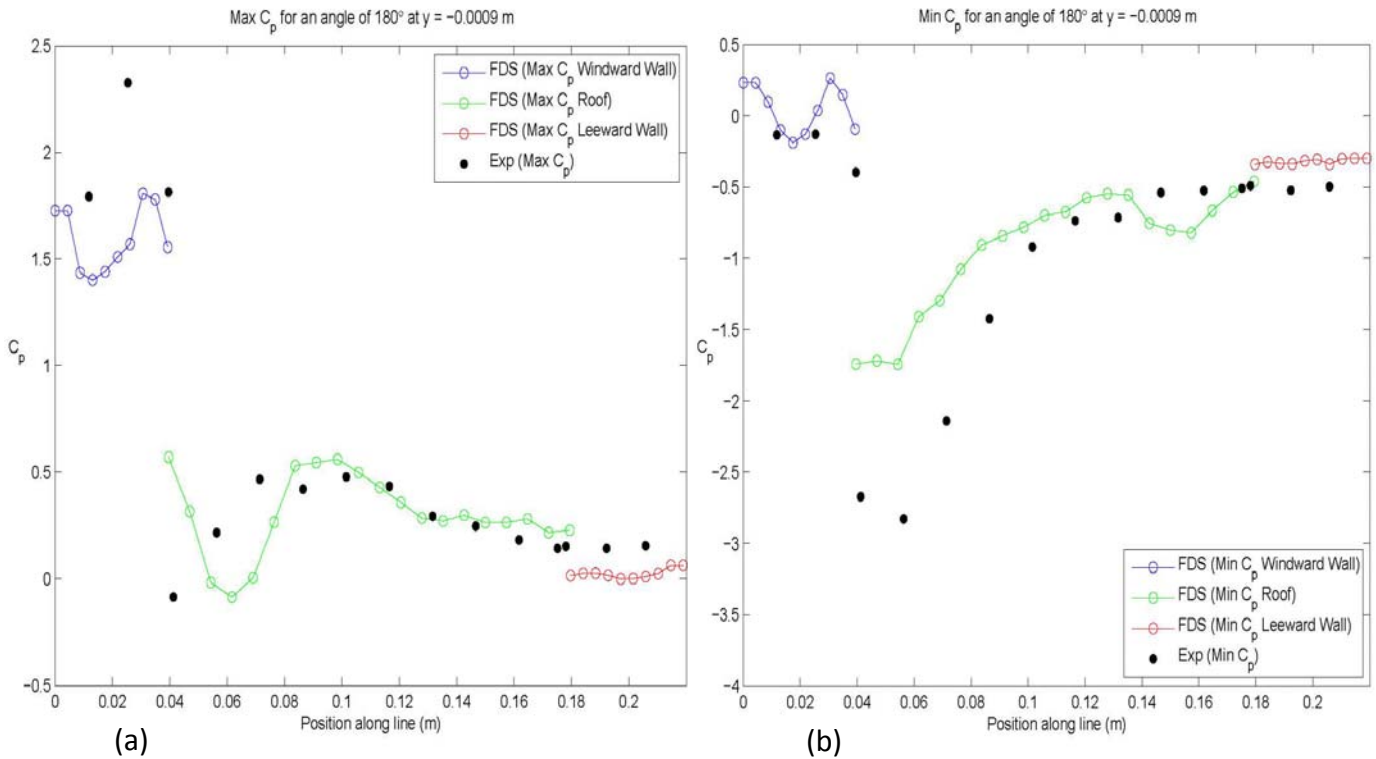
Figure 7 FDS and experimental (a) maximum pressure and (b) minimum pressure data for the line of devices at y = -0.0009 m in the 180° case.

3.3 Turbulence Model

Two different turbulence models were used in FDS simulations: Deardorff and Dynamic Smagorinsky turbulence models [5, 6]. The default turbulence model in FDS is the Deardorff turbulence model. Mean pressure coefficient data output for the perpendicular flow cases from FDS were compared with experimentally obtained values to determine which of these models are more accurate. The Smagorinsky constant was varied from 0.05 to 0.20 (default value). The results show that the Smagorinsky constant had little effect on the FDS output of pressure coefficients and that there were slight differences between the two turbulence models. A detailed analysis showed that the Deardorff model performed better overall, especially for the regions over the roof of the building. An example plot of the effects of the two turbulence models on computed pressure coefficients is shown in Figure 8(a). Figure 8(b) shows the influence of the mesh discretization level on the computed pressure coefficient values for cases run with Deardorff turbulence model. It is clear from this plot that the finer mesh generally yields results closer to the experimental values.
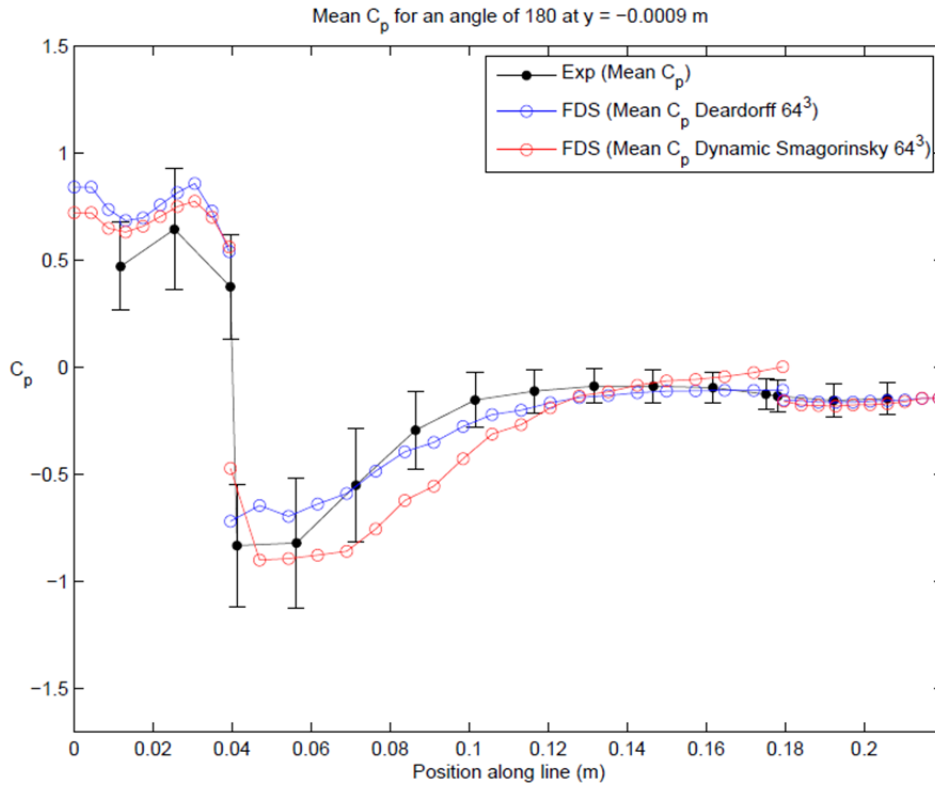
Figure 8 (a) FDS and experimental mean pressure data for the line of devices at y = -0.0009 m in the 180° case for the Deardorff and Dynamic Smagorinsky turbulence models. This plot is an example of the Deardorff model outperforming the Dynamic Smagorinsky model, particularly for the roof.
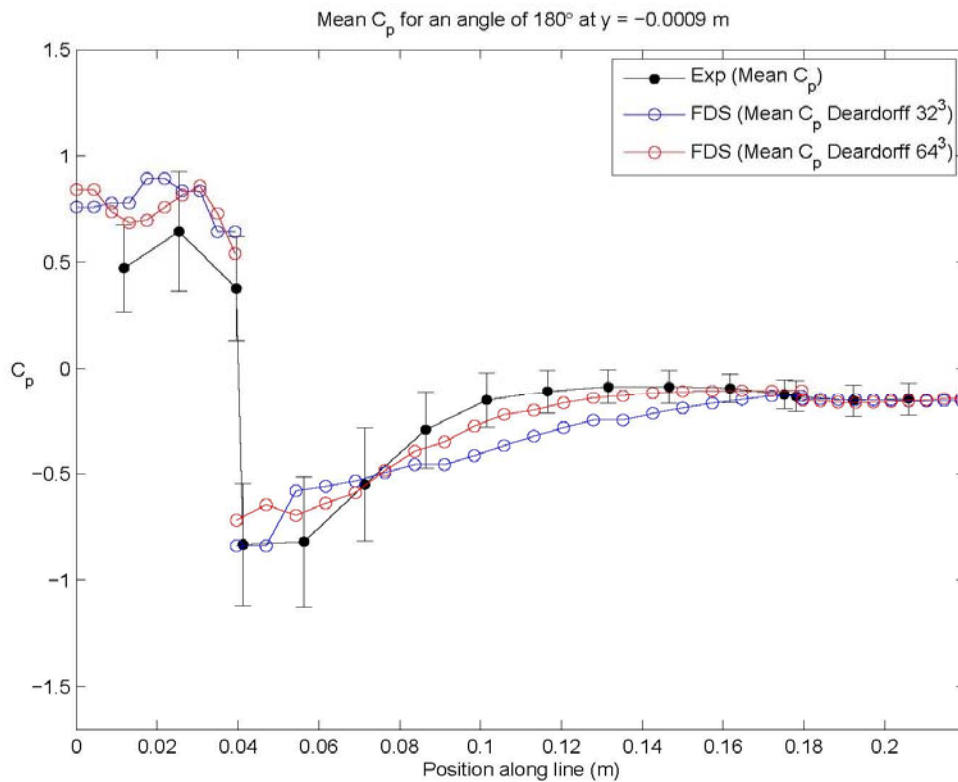

Figure 8(b) FDS and experimental mean pressure data for the line of devices at y = -0.0009 m in the 180° case for the Deardorff turbulence models for two levels of discretization. The plot shows that the finer mesh yields results closer to the experimental data.

3.4 Pressure Spectra and Spatial Coherence

The atmospheric turbulence structure is defined in terms of fluctuating velocity spectra and spatial coherence. A normalized pressure spectrum plot on the windward wall shows a steady decrease with the increase in frequency (Figure 9). The FDS output shows good agreement with experimental results. It is clear that the peak occurs at a low frequency; both the experimental and simulated results show similar behavior.

Spatial coherence provides a useful insight into the turbulence structure and is best described by statistical methods employing integral scale length, cross-spectra, and coherence measures. Quantitative estimates of the effect of spatial turbulence can be determined from the correlation coefficient and coherence function. The spatial coherence between two points on the windward wall is plotted for the FDS (for both fine and coarse mesh simulations) along with experimental data (Figure 10). The discrepancy between experimental and simulated results is evident. However, FDS simulations with fine mesh tend to match experimental results reasonably well especially at higher frequencies. The simulated results show that spatial coherence calculation is sensitive to the selection of the level of discretization and a much finer discretization is expected to yield better computed results, especially at higher frequencies. It can be seen that frequencies close to zero, FDS results show a low coherence for finer mesh case. In reality, this value should be close to unity. Also, coherence values with coarse mesh are high at higher frequencies. The reason behind this is not clear. More detailed investigation is needed to understand this behavior.
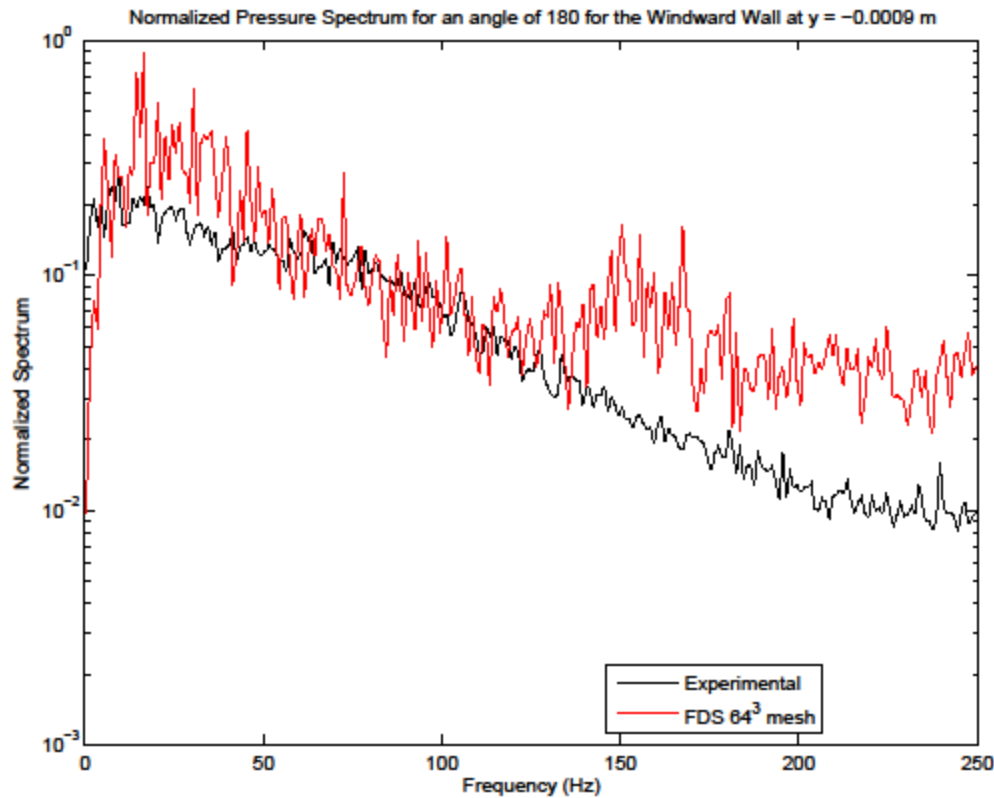

Figure 9 FDS and experimental averaged pressure spectra for the windward wall on the line of devices at y = -0.0009 m in the 180° case. This plot shows that the FDS and experimental spectra are well matched.
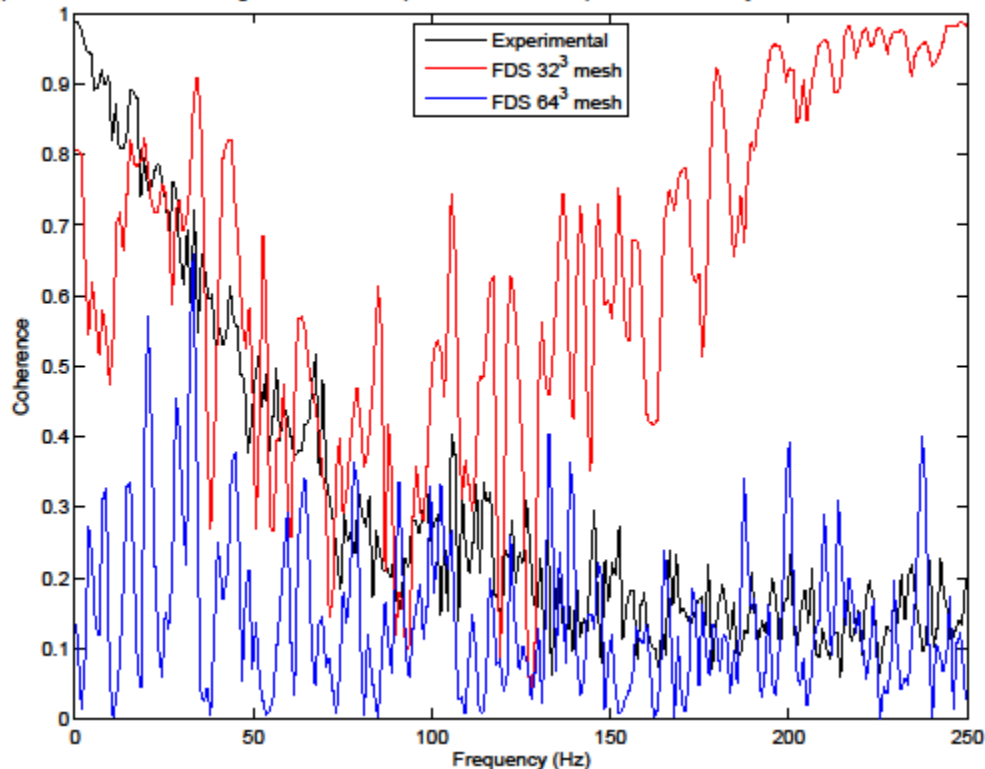
Figure 10 FDS and experimental spatial coherence for two points on the windward wall on the line of devices at y = -0.0009 m in the 180° case. This plot shows that the FDS and experimental spatial coherences are not as well matched as the spectra.

3.5 Computational Issues

As mentioned before, FDS simulation was run with 8 meshes that were used to discretize the computational domain and comprised 32^3 or 64^3 cells per mesh, depending on the resolution. This corresponds to either 262,144 or 2,097,152 cells in the computational domain for the two mesh resolutions. As a result, the calculations for each mesh were performed on separate processors to prevent excessive simulation run times.

FDS simulations were run on a Linux Cluster comprising 1 Head Node and several Compute Nodes with multiple Intel Xeon DP E5620 Processors per Node. Even with 8 processors, the final simulations could take anywhere from 1 to 8 days to run. The amount of output data written had a strong influence on the final clock time of simulation.

On the average, FDS simulations with 32^3 cells per mesh took about 1-2 days while those with 64^3 cells per mesh took about 3-4 days to run for a total simulated time of 5 seconds.

4. SUMMARY

FDS has been successfully used to simulate wind tunnel flow and pressures on a low rise building. FDS simulated mean pressure coefficient results compared reasonably well with experimentally measured values. However, FDS results did not match the maximum and minimum values of the pressure coefficient. This was true for all angles of attack.

FDS predictions of the velocity spectrum and turbulence intensity showed that the turbulence model used in FDS provides a reasonable prediction of the wind flow in the wind tunnel. The mean inlet velocity profile computed along the length of the computational domain matched the measured wind velocity profile.

FDS provided a good prediction of the turbulence structure near the vicinity of the model building both in terms of pressure spectrum and spatial coherence. Computed results showed good agreement with measured data, especially at lower frequencies.

The study indicates that FDS has the potential for adaptation to solving wind engineering problems. However, simplifications of the computational mesh, boundary conditions, and parallel processing are necessary to obtain simulated results within a reasonable clock time.

5. ACKNOWLEDGMENTS

6. REFERENCES

1. J. Floyd, G. Forney, S. Hostokka, T. Korhonen, R. McDermott, K. McGrattan, and C. Weinschenk, "FDS 6 User Guide", 6th edition, NIST Special Publication 1019, Gaithersburg, Maryland, April 2013.

2. T. C. E. Ho, D. Surry, and D. P. Morrish, "NIST/TTU Cooperative Agreement – Windstorm Mitigation Initiative: Wind Tunnel Experiments on Generic Low Buildings," Univ. of Western Ontario, London, Ontario, Canada, Rep. BLWT-SS20-2003, May 2003 http://fris2.nist.gov/winddata/uwo-data/blwt-ss20-2003.pdf.

3. N. Jarrin. Synthetic Inflow Boundary Conditions for the Numerical Simulation of Turbulence. PhD thesis, The University of Manchester, Manchester M60 1QD, United Kingdom, 2008. 60, 61.

4. E. Simiu and R.H. Scanlan, "Wind Effects on Structures: Fundamentals and Applications to Design". 3rd Edition, John Wiley and Sons, New York, 1996.

5. J.W. Deardorff, "Numerical Investigation of Neutral and Unstable Planetary Boundary Layers", Journal of Atmospheric Sciences, 29:91–115, 1972.

6. J. Smagorinsky, "General Circulation Experiments with the Primitive Equations. I. The Basic Experiment", Monthly Weather Review, 91(3):99–164, March 1963.